

Validated Uncertainty Propagation for Estimation and Measure Association, Application to Satellite Tracking

Charlotte Govignon¹, Elliot Brendel² and Julien Alexandre Dit Sandretto³

¹*École des Ponts ParisTech, Cité Descartes, 6 et 8 avenue Blaise Pascal, 77420 Champs-sur-Marne, France*

²*Thales Land and Air Systems, Paris, France*

³*ENSTA Paris, Institut Polytechnique de Paris, 828 Boulevard des Maréchaux, Palaiseau 91120, France*

Keywords: Estimation, Association, Intervals, Contractors, Satellite Tracking, Radar.

Abstract: In this paper, we present a new uncertainty propagation algorithm based on interval arithmetic, and its applications for space surveillance. Using validated simulation, the goal is to explore the benefits of a set-based approach of estimation and data association for satellite tracking. The presented algorithm capitalises on the position measures of a satellite to improve its estimation and reduce uncertainties on its trajectory. Our approach also contributes to data association by computing the precision required for a measure to belong to a given track with confidence-levels. This paper illustrates the contributions of this new algorithm with several scenarios of orbit determination and satellite tracking and their numerical simulations.

1 INTRODUCTION


Space surveillance of low-earth objects has become a major issue, notably in a military context, and can be addressed by ground radars, providing detection and tracking of satellites of interest. In order to perform the tracking of these objects, two crucial steps must be accomplished: estimation and association.


The estimation problem consists in using the information provided by a set of measures and their respective uncertainties to compute the state of a dynamical system, for instance position and velocity coordinates, while minimizing the state uncertainty. Within this context, the simulation of the considered dynamical system is often needed and can be used to improve the estimation accuracy. The simulation of a dynamical system usually requires the computing of the solution of a differential equation representing its dynamics. An other issue in the estimation problem occurs when multiple systems evolve in the observed environment. In that case, the sensor providing the measures can produce data coming from different sources. Hence, it is essential to filter the measures between those coming from the considered system and the others, in order to prevent the estimate


from corruption. This issue is called association.

Data association techniques can be divided in two categories. First, instantaneous decision techniques which assign a measure to an object at the time when the measure is generated. In these techniques, Nearest Neighbor (NN) (Blackman and Popoli, 1999) approaches consist in assigning the considered measure to its closest object by computing a chosen quantity representing a distance between the measure and its surrounding objects. Such quantities can be deterministic (e.g. the Cartesian distance) or statistical (e.g. the Mahalanobis distance (Verhagen and Teunissen, 2017)). When multiple measures and multiple objects are considered at the same time, Global Nearest Neighbor (GNN) approaches (Blackman and Popoli, 1999) use optimization techniques such as the Hungarian method (Mills-Tettey et al., 2007) to maximize association scores between measures and objects. Usually, NN and GNN's efficiency decreases when the number of measures and objects increases.

Probabilistic Data Association (PDA) (Blackman and Popoli, 1999; Bar-Shalom and Tse, 1975; Fortmann et al., 1983) approaches are instantaneous decision techniques which consist in the computation of the probability of each association hypothesis and the selection of a subset of these hypotheses. Then, a combination of the selected hypotheses is evaluated, assigned to an object and used to improve its

^a <https://orcid.org/0009-0003-7703-0785>

^b <https://orcid.org/0000-0002-0458-4993>

^c <https://orcid.org/0000-0002-6185-2480>

estimate. This approach is usually suited for environments with risk of confusion between multiple objects. On the other hand, delayed decision techniques wait until several measures are generated to perform an association taking into account the information of the batch of the measures. For example, Multi-Hypothesis Tracking (MHT) (Blackman and Popoli, 1999; Reid, 1979) approaches consist in building and updating a set of association hypotheses until their respective estimated probabilities lead to the removal of one of the previously considered hypotheses. These techniques are efficient but show high combinatorial cost. Furthermore, the long time needed to take a decision can be a drawback in operating environment.

Other delayed decision approaches consist in the combination of gating (Collins and Uhlmann, 1992) and estimation (Verhagen and Teunissen, 2017; Vallado, 2001; Julier and Uhlmann, 2004) methods. Gating consist in selecting a subset of measures verifying a condition (e.g. all the measures whose distance with the estimate is under a chosen threshold). Then, estimation techniques, such as Extended Kalman Filter (Blackman and Popoli, 1999; Verhagen and Teunissen, 2017; Vallado, 2001; Julier and Uhlmann, 2004) or Least Squares optimization (Verhagen and Teunissen, 2017; Vallado, 2001; Gill and Murray, 1978) are used to update the estimate with the subset of selected measures. At last, the new estimate is used to realize a final gating step, and the new selected measures are considered as assigned to the object.

Most of the described association techniques are probabilistic approaches, and they are often based on the hypothesis that Gaussian distributions describe well enough the several uncertainties (from the measures and the estimates) all along the trajectories of the considered objects. Yet, a ground radar can only provide measures for low-earth satellites when these objects are in its field of view. Therefore, due to earth rotation and satellite dynamics (see 2.2), measures of an observed satellite can be spaced out by several hours, causing a loss of precision in the estimate of the satellite state, leading to increased uncertainties and, potentially, confusion with other objects. Moreover, it has been documented that a Gaussian distribution propagated along an orbital trajectory can lose its Gaussian nature (Horwood and Poore, 2014), in particular with large uncertainties, for example when the object generated a limited number of measures. In that case, the previously described techniques become unsuitable. Conversely, deterministic set-based propagation and association approaches, using classical set theory functions such as intersection, inclusion and contractors, provide a guaranteed enclosure of all the possible values of the objects states. The obtained

enclosures can be used to decide, with guarantee, if a measure belongs to an object or not. Such techniques are therefore relevant in a space surveillance context. The approaches developed in this paper are applied to association, estimation and tracking of satellites observed by a ground radar. Performances and benefits of these approaches are discussed in connection to this space surveillance application.

2 ORBIT DETERMINATION

2.1 Orbit Description

The state of a satellite is usually given with its vectors of position and speed. These six coordinates can be expressed in earth-centered Cartesian references such as *Earth-Centered Inertial* (ECI) or *Earth-Centered Earth-Fixed* (ECEF). Alternatively, it can be convenient to describe a satellite state in the *Keplerian* or the *Equinoctial* frames (Vallado, 2001), especially when the dynamics are unperturbed, since these frames provide a more direct handling of the parameters of the ellipse. *Modified equinoctial elements* (Walker et al., 1985) (mEOE) are derived from Keplerian elements $(a, e, i, \Omega, \omega, \theta)$ as follows:

$$\begin{cases} p = a(1 - e^2), L = \Omega + \omega + \theta \\ f = e \cos(\omega + \Omega), g = e \sin(\omega + \Omega) \\ h = \tan\left(\frac{i}{2}\right) \cos \Omega, k = \tan\left(\frac{i}{2}\right) \sin \Omega \end{cases} \quad (1)$$

where a denotes the semi-major axis, e the eccentricity, i the inclination, Ω the longitude of the ascending node, ω the argument of the periapsis, θ the true anomaly. The element p is called the semi-parameter and the element L the true longitude. This reference is useful for trajectory analysis because of the stability of the state components in time.

2.2 Dynamics of a Satellite

The dynamics of a satellite in mEOE is given by Equation (2) (Walker et al., 1985):

$$\begin{cases} \dot{p} = \frac{2p}{w} \sqrt{\frac{p}{\mu}} \Delta_r \\ \dot{f} = \sqrt{\frac{p}{\mu}} \left(\frac{((w+1) \cos L + f) \Delta_r - g j \Delta_n}{w} + \Delta_r \sin L \right) \\ \dot{g} = \sqrt{\frac{p}{\mu}} \left(\frac{((w+1) \sin L + g) \Delta_r + f j \Delta_n}{w} - \Delta_r \cos L \right) \\ \dot{h} = \sqrt{\frac{p}{\mu}} \frac{s^2 \Delta_n}{2w} \cos L, \dot{k} = \sqrt{\frac{p}{\mu}} \frac{s^2 \Delta_n}{2w} \sin L \\ \dot{L} = \frac{\sqrt{\mu p}}{r^2} + \frac{1}{w} \sqrt{\frac{p}{\mu}} (h \sin L - k \cos L) \Delta_n \end{cases} \quad (2)$$

where $w = 1 + f \cos L + g \sin L$, $s^2 = 1 + h^2 + k^2$, and $j = h \sin L - k \cos L$. Δ_r , Δ_r and Δ_n are the non-two-

body perturbations in the radial, tangential and normal directions, respectively. These perturbations aggregate all other orbital perturbations acting on the satellite, like the J_k effects ($k \in \{2, 3, \dots\}$) which come from the non-sphericity of the Earth, or the atmospheric drag for instance. With only J_2 effects, which induce the strongest perturbation from the non-sphericity of the Earth, the perturbations are:

$$\begin{cases} \Delta_r^{J_2} = -\frac{3\mu J_2 R_e^2}{2r^4} \left(1 - \frac{12j^2}{s^4}\right) \\ \Delta_t^{J_2} = -\frac{12\mu J_2 R_e^2}{r^4} \left(\frac{j(h \cos L - k \sin L)}{s^4}\right) \\ \Delta_n^{J_2} = -\frac{6\mu J_2 R_e^2}{r^4} \left(\frac{(1-h^2-k^2)j}{s^4}\right) \end{cases} \quad (3)$$

where J_2 is the second order zonal coefficient, R_e the earth radius, μ the standard gravitational parameter and $r = \frac{p}{w}$ is the radius. Without perturbations, all equinoctial elements are constant except the true longitude L which is close to linear (see Equation (2)).

2.3 Satellite Tracking by Ground Radar

In order to detect new objects, a ground radar scans periodically the space. Then, measure association is performed: every produced measure is compared to the estimates of known objects in order to decide if the measure was generated by a known object or by a previously unknown one. If the measure belongs to a known object, its estimate is updated and improved by the information of the measure. If the measure belongs to a new object, an estimate of this object is computed and the object will be considered as known for the future measures performed by the radar.

In this paper, the considered radar produces measures of the position of detected objects in the ECI frame. This simplification is justified by the fact that measures performed in a Radar frame, such as Azimuth-Elevation-Range, can easily be converted in a Cartesian frame using classical formulas (Vallado, 2001). The measures provided by the radar come with a covariance matrix, also in ECI, representing the uncertainties of the associated measures. Mathematically, each of these measures can be modelled by a random variable $X_{\text{mes}} \in \mathbb{R}^3$ normally distributed with mean $x_{\text{true}} \in \mathbb{R}^3$ (the true position of the satellite in the ECI frame) and covariance $P \in \mathbb{R}^{3 \times 3}$ (depending on the radar performances and the satellite position).

3 SET-BASED PROPAGATION

One of the most used tool to handle uncertainty enclosed by sets is the interval arithmetic.

3.1 Interval Arithmetic

By using *interval arithmetic* (Jaulin et al., 2001), uncertainties can be represented with a deterministic set-based approach. An interval $[a] = [\underline{a}, \bar{a}]$ defines the set of $a \in \mathbb{R}$ such that $\underline{a} \leq a \leq \bar{a}$. \mathbb{IR} denotes the set of all intervals over \mathbb{R} . The extension of mathematical operators for interval arithmetic is defined as $[a] * [b] = \{a * b \mid a \in [a], b \in [b]\}$ with $*$ a binary operator on real numbers. Such operations can sometimes be expressed via the bounds of the intervals, but not always. For instance, the sum of two intervals $[a]$ and $[b]$ gives $[\underline{a} + \underline{b}, \bar{a} + \bar{b}]$. Elementary functions can also be extended to interval arithmetic. A *tube* denotes the image of a function $f : t \in \mathbb{R} \mapsto [f(t)] \in \mathbb{IR}$. Furthermore, the Cartesian product of n intervals is called an interval vector or a *box* $[a] \in \mathbb{IR}^n$.

An *interval contractor* associated to the set $A \subset \mathbb{R}^n$ is an operator $C : [a] \in \mathbb{IR}^n \mapsto C([a]) \in \mathbb{IR}^n$ satisfying the contractance property ($C([a]) \subseteq [a]$) and the completeness property ($C([a]) \cap A = [a] \cap A$). Associated to a *constraint*, a contractor allows to reduce the size of an interval while preserving the subset of real numbers verifying the constraint.

3.2 Validated Simulation

Numerical integration consists in approximating a solution of an ordinary differential equation (ODE), $\dot{y} = f(y)$, using an integration scheme (such as Euler or Runge-Kutta). Interval arithmetic can be applied to numerical integration in order to provide validated numerical integration methods, also named reachability analysis or guaranteed simulation.

Such validated integration methods use a guaranteed integration scheme, providing a discretization of time, $t_0 \leq \dots \leq t_{\text{end}}$, and a computation of enclosures of the set of states of the system $y_0, \dots, y_{\text{end}}$.

A guaranteed integration scheme consists in an integration method $\Phi(f, y_j, t_j, h)$, approximating the exact solution $y(t_{j+1}; y_j)$, i.e., $y(t_{j+1}; y_j) \approx \Phi(f, y_j, t_j, h)$, where y_j is an initial value, t_j the initial time, and h the step-size ($t_{j+1} = t_j + h$), and a truncation error function $\text{LTE}_\Phi(f, y_j, t_j, h)$, such that $y(t_{j+1}; y_j) = \Phi(f, y_j, t_j, h) + \text{LTE}_\Phi(f, y_j, t_j, h)$. Taking into account the inaccuracy of the used integration scheme, in contrast with usual integration methods, a validated numerical integration method is a two-step method which, firstly, computes an enclosure $[\tilde{y}_j]$ of the solution over the time interval $[t_j, t_{j+1}]$ to bound $\text{LTE}_\Phi(f, y_j, t_j, h)$, then, computes a tight enclosure of the solution for the final time instant t_{j+1} . Multiple methods exist to perform these steps, such as Taylor series and Runge-Kutta, see (Nedialkov et al., 1999;

Alexandre dit Sandretto and Chapoutot, 2016) and the references therein for more details. The step-size can be fixed (h is a constant) or adaptive (h is computed at each step). Finally, functions R and \tilde{R} are provided by validated numerical integration methods

$$R: \begin{cases} \mathbb{R} & \rightarrow \mathbb{I}\mathbb{R}^n \\ t & \mapsto [y] \end{cases}, \tilde{R}: \begin{cases} \mathbb{I}\mathbb{R} & \rightarrow \mathbb{I}\mathbb{R}^n \\ [t, \bar{t}] & \mapsto [\bar{y}] \end{cases} \quad (4)$$

with for a given t_i , $R(t_i) = \{y(t_i; x_0) : \forall y_0 \in [y_0]\} \subseteq [y]$, and $\tilde{R}([t, \bar{t}]) = \{y(t; y_0) : \forall y_0 \in [y_0] \wedge \forall t \in [t, \bar{t}]\} \subseteq [\bar{y}]$.

3.3 Confidence Contractor

Intervals and probabilities are strongly connected. Indeed, the universe of a distribution is an interval, and a given confidence level is associated to a confidence interval. A *confidence interval* is a set \mathcal{S} for which the probability of the given random variable to be in this set is equal to the given probability P . In other words, let \hat{x} be a single observed sample of the quantity X . In statistics, an observed data allows to compute a confidence interval (Neyman, 1937), that is to say an interval which may contain the actual value, with respect to a given confidence level. For example, considering a confidence level $CL = 95\%$, one can define the confidence interval $C_{95\%}$. This interval can be obtained by observation (statistical approach) or with the help of a known distribution (probabilistic approach). A new measure \hat{x} coming from the (same) experiment will be in the associated confidence interval such that $\hat{x} \in C_{95\%}$ 95% of the time.

We use in our algorithm the confidence contractor proposed in (Alexandre Dit Sandretto, 2019):

$$Cbc([x]|f_X, cc): \begin{cases} \mathbb{I}\mathbb{R} & \rightarrow \mathbb{I}\mathbb{R} \\ [x] & \mapsto [x] \cap [y] \end{cases} \quad (5)$$

with $[y]$ defined such that $Pr(x \in [y]) = \int_{[y]} f_X(x) dx = cc$ ($[y]$ is the confidence interval), $Pr(x \in [y])$ stands for “probability that x is in $[y]$ ”, with x following the distribution f_X , and cc being the confidence coefficient ($0 \leq cc \leq 1$). For example, $cc = 0.68$ for a 68% confidence level. In the domain of ODEs, confidence contractor has been used to produce potential clouds (Fuchs and Neumaier, 2009) in (Alexandre Dit Sandretto, 2019).

4 ASSOCIATION, ESTIMATION

Based on interval arithmetic and validated simulation, our approach uses measures of the satellite’s position to improve the estimation of its trajectory and rule out incompatible measures and tracks.

4.1 Definition of Measures

To measure a quantity $x_{\text{true}} \in \mathbb{R}^n$, instruments provide a measure with its associated uncertainty, in either a deterministic (Equation (6)) or a probabilistic (Equation (7)) approach. In the deterministic case, the measure $x_{\text{mes}} \in \mathbb{R}^n$ and uncertainty $\Delta x_{\text{mes}} \in \mathbb{R}_+^n$ generate an interval vector that necessarily includes x_{true} :

$$x_{\text{true}} \in [x_{\text{mes}} \pm \Delta x_{\text{mes}}]. \quad (6)$$

In the probabilistic approach, the measure is represented as a random variable X_{mes} normally distributed with mean x_{true} and covariance $P \in \mathbb{R}^{n \times n}$:

$$X_{\text{mes}} \sim \mathcal{N}(x_{\text{true}}, P). \quad (7)$$

In the probabilistic approach, the uncertainty is carried by the covariance matrix P . Usually, the probabilistic approach is preferred to represent uncertain measures. However, the downside of this method is its lack of accuracy to describe rare events and singularities that have a low probability to be drawn. In contrast, the deterministic, or set-based approach allows to take the entire measure interval into consideration, which is significantly more robust with worst case scenarios. For this reason, we choose to consider measures as real valued intervals.

For our application, the ground radar provides probabilistic uncertainties. Thus, a conversion from the uncertainty covariance P to a deterministic uncertainty Δx_m is required and explained in section 5.

4.2 Representation with Contractors

Two cases are considered: an ideal case where complete observation of the system is provided and a more realistic case where this observation is only partial.

Complete Observation of the System

Consider a dynamical system of state $x_{\text{true}}(t) \in \mathbb{R}^n$ at time $t \in \mathbb{R}$, following the dynamics $\dot{x}_{\text{true}} = f(x_{\text{true}})$ with $f: \mathbb{R}^n \rightarrow \mathbb{R}^n$. The state is measured with a deterministic approach, as in Equation (6).

On one hand, measures of the dynamical system provide an enclosure of the state. At time t , the measure $x_t^m \in \mathbb{R}^n$ and its associated uncertainty $\Delta x_t^m \in \mathbb{R}_+^n$ are obtained, and give the following inclusion:

$$x_{\text{true}}(t) \in [x_t^m \pm \Delta x_t^m]. \quad (8)$$

On the other hand, validated numerical integration of the dynamical system provides an interval estimate encompassing the state of the system. At time t , the estimate $[\hat{x}_t]$ of the system is given by:

$$[\hat{x}_t] := R(t) \in \mathbb{I}\mathbb{R}^n, \quad (9)$$

where $R(\cdot)$ is defined in Equation (4), and $R(t_0) = x_0$ with x_0 the initial value of the system, at time t_0 . The true state at time t is also included in $[\hat{x}_t]$:

$$x_{\text{true}}(t) \in [\hat{x}_t]. \quad (10)$$

Using Equations (8) and (10), one concludes that the state of the dynamical system is included in the intersection of the measure and the estimate:

$$x_{\text{true}}(t) \in [x_t^m \pm \Delta x_t^m] \cap [\hat{x}_t]. \quad (11)$$

Further, if the exact time $t \in \mathbb{R}$ of the measure is not known precisely, it can be approximated by a time interval. Assume that the exact time t is bounded by $\underline{t} \leq t \leq \bar{t}$, then instead of using $R(\cdot)$ to provide the estimate as in Equation (9), the function $\tilde{R}(\cdot)$ generates an estimate $[\hat{x}_t] := \tilde{R}(t) \in \mathbb{I}\mathbb{R}^n$, that takes account of the uncertainty on the time of the measure.

Partial Observation of the System

In some cases, the intervals measured from the dynamical system are only partial, or in a different reference frame. Let us consider that the sensor can only make observations $y_t^m \in \mathbb{R}^p$ of the system $x_{\text{true}}(t) \in \mathbb{R}^n$, with $p \leq n$. A function $g : \mathbb{R}^n \rightarrow \mathbb{R}^p$ gives the constraint $y_t^m = g(x_{\text{true}}(t))$, or equivalently

$$g(x_{\text{true}}(t)) - y_t^m = 0, \quad (12)$$

which represents the compatibility of the system x_{true} with the measure y_t^m at time t . If a measure y_t^m does not verify this constraint, then it cannot come from the system x_{true} . Further, if the measure y_t^m comes from the system x_{true} , the constraint in Equation (12) provides more information on the state of system $x_{\text{true}}(t)$.

Given a partial measure interval $[y_t^m] \in \mathbb{I}\mathbb{R}^p$ and an estimated interval $[\hat{x}_t] \in \mathbb{I}\mathbb{R}^n$ of a system at time t , the interval counterpart of Equation (12) is as follows:

$$\begin{cases} g([\hat{x}_t]) \subset [y_t^m] \\ g^{-1}([y_t^m]) \subset [\hat{x}_t] \end{cases} \quad (13)$$

The smallest subset of $[\hat{x}_t]$ that respects Equation (13) is computed with a forward-backward contractor (Benhamou F. and J-F., 1999).

As a result, interval contractors allow to use the partial information provided by the measures when the measures are only partial and cannot be used to directly intersect the estimated interval (Equation (11)).

4.3 Association of Measures

Comparing the estimate of a dynamical system with new measures helps reducing the uncertainty of the estimate and contributes to the association issue.

Our algorithm (see Algorithm 1) ensures that a measure is compatible with the simulated dynamical system to associate them. Since the simulation is validated, the estimated interval vector necessarily includes every possible states of the satellite. So, if a measure interval does not intersect with the simulation interval associated with that instant, this necessarily means that the measurement is incompatible with that track. Nonetheless, it is possible that certain measures give a non-empty intersection with the simulation estimate, but do not really correspond to the same system. Hence the significance of introducing confidence levels in the measurements.

Data: Estimate $[\hat{x}_t]$, Measure $[x_t^m \pm \Delta x_t^m]$

Result: Association decision at time t

if $[\hat{x}_t] \cap [x_t^m \pm \Delta x_t^m] \neq \emptyset$ **then**

 Association because of compatibility;

 Improvement of the estimate:

$[\hat{x}_t] \leftarrow [\hat{x}_t] \cap [x_t^m \pm \Delta x_t^m]$;

else

 Incompatibility, no association ;

end

Algorithm 1: Measure Association.

Once the algorithm ruled out incompatible measures, it uses the additional information of the measure to increase the precision on the state of the dynamical system. The system is included in both the measure interval and the estimated interval. Consequently, it is included in their intersection. This gives an upgrade of the estimate by reducing the uncertainty on the state of the system after the measure.

5 RESULTS

The presented method has been implemented in the Dynlbex framework (Alexandre dit Sandretto and Chapoutot, 2016). It provides interval arithmetic tools such as contractors and offers a validated numerical integration procedure based on Runge-Kutta methods with adaptive step-size. The presented simulations were computed using the *implicit midpoint* method. The local truncation error was set to 10^{-7} . This choice of parameters granted a good trade-off between computation time and precision.

The objects were simulated in mEOE. The semi-parameter p was normalised by the Earth radius and the time unit for the integration was hours instead of seconds to facilitate the computations. The measures provided by the ground radar were on the position of the satellite, in the Cartesian reference ECI.

The initial estimate of each simulated satellite is supposed to be normally distributed with a mean vec-

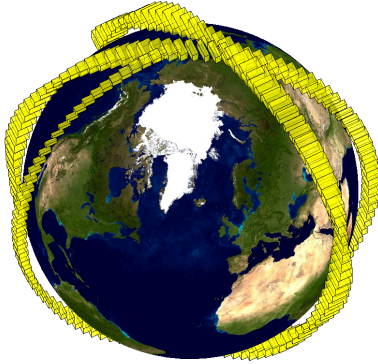


Figure 1: Simulation of a trajectory of a satellite for 6 hours, represented by the boxes of uncertainties on its position.

for x_0 and a covariance matrix P . x_0 depends on the scenario and P is chosen diagonal such that $P_{11} = 594.817$, $P_{66} = 1.258 \cdot 10^{-11}$ and $P_{ii} = 5.948 \cdot 10^{-12}$ for $i = \{2, \dots, 5\}$. This covariance matrix is representative of the uncertainties on the state of a satellite after a few measures. It is satisfactory to demonstrate the contribution of our algorithm but in operating environment, distinct covariance matrices for the satellites of interest would be considered, depending on the measures used to compute their estimate, and a given time at which the matrices are evaluated.

Then, a reference box is computed using the confidence contractor of Equation (5) with a 99% confidence level: $\Delta x_{\text{ref}} = [-x_{\text{ref}}, +x_{\text{ref}}]$ where $x_{\text{ref}} = (100, 10^{-6}, 10^{-6}, 10^{-6}, 10^{-6}, 1.45408 \cdot 10^{-5})$. This represents an uncertainty of ± 100 meters on the semi-parameter p , and approximately ± 100 meters on the arc of circle represented by the true longitude L when the altitude of the satellite is 500 kilometers.

The potential clouds associated to the 5% and 95% confidence levels are given by $\Delta x_{5\%} = 0.21\Delta x_{\text{ref}}$ and $\Delta x_{95\%} = 0.645\Delta x_{\text{ref}}$. Then, with x_0 an initial state of a satellite, the initial box associated to the $n\%$ potential cloud ($n = 5, 95$) is given by $x_0 + \Delta x_{n\%}$.

5.1 Sc. 1: Propagation of Uncertainties

The first scenario consists in the propagation of the 5% and 95% potential clouds of a satellite for 6 hours, using the function R defined in Equation (4).

Figure 2 shows the results on the components p and L . For an easier comparison between the two potential clouds, the intervals are translated using the center of the 95% interval. After 6 hours, the 95% potential cloud associated to the semi-parameter p is about 600 meters wide, three times greater than the 5% potential cloud. Along the propagation, the order of magnitude stays the same for the two potential clouds associated to p . In contrast, the widths of

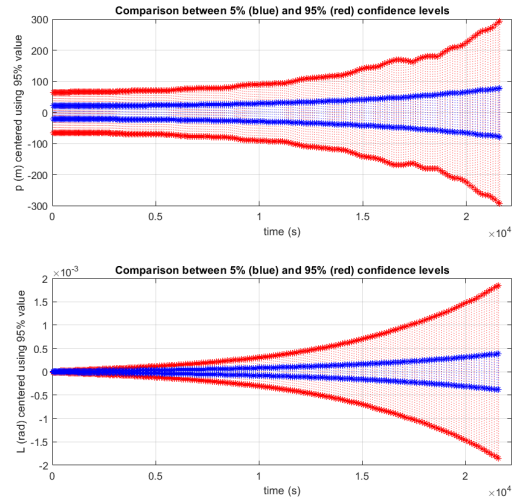


Figure 2: Propagation of the 5% (blue) and 95% (red) potential clouds on the p and L components.

the potential clouds associated to L increase faster and after 6 hours, the circular arcs corresponding to such intervals are about 7 kilometers for the 5% potential cloud and 27 km for the 95% potential cloud. The specificity of the component L is discussed in 5.2. Finally, it can be observed that, as expected, the 5% intervals are always included in the 95% intervals.

5.2 Sc. 2: Effect of Measures on Estimation Uncertainties

In this scenario, a ground radar provided an estimate of the state of the satellite at an initial time, and propagated its estimate for 12 hours with the function R (see Equation (4)) before being able to measure its position again. When the satellite gets in the scope of the radar again, a series of 10 measures of its position over 5 minutes are taken. Using our algorithm, these measures are added to the estimation process.

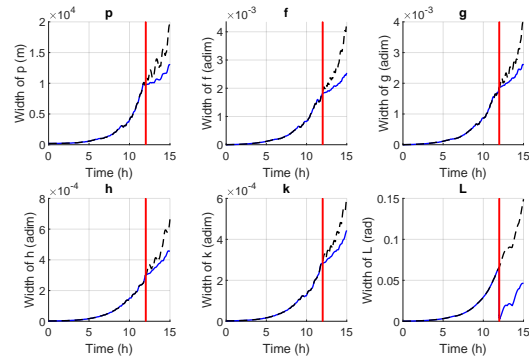


Figure 3: Propagation of the uncertainties, with (blue) and without (black) addition of 10 measures after 12 hours (red).

Figure 3 shows that L is significantly impacted by the series of measures, in comparison to other components of the state of the satellite. Indeed, the uncertainty over L drops with the addition of measures. The precision of the other components also improves after the addition of measures, compared to the scenario where no measure was added. This results from the precision gain of L spreading to the other state's components through the dynamics equations.

The impact of the measures on the component L is due to L encoding the position of the satellite along the orbit described by the five other components. Therefore, this component is strongly linked to the position of the satellite, hence the steep decrease of its uncertainties when a position measure is added. Further, the true longitude L is the component which is the most subject to variations over time, since it is the only non-constant one when the dynamics is unperturbed (see Equation (2)). Therefore, it makes the propagated uncertainties grow faster for the true longitude L . By focusing on the impact of each measure of the series on L , it gives Figure 4.

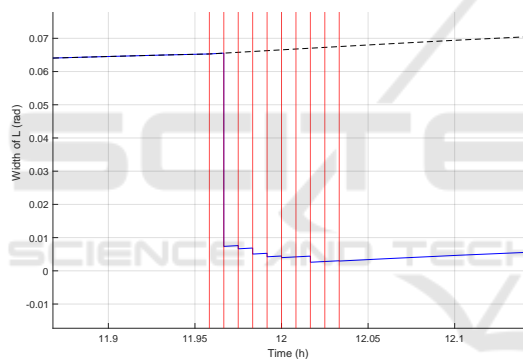


Figure 4: Focus on the effect of each measure on L .

Figure 4 helps raising two points. First, not every measure helps improving the estimate of the satellite's position. Here, the first measure of the series does not reduce the estimate's uncertainty. Mathematically, it means that the estimation interval was included in the measure interval. The radar is not precise enough to bring new information. Secondly, most of the precision given by the series of measures comes from the first measures. This could allow computing the number of measures that would be necessary to achieve a certain precision on the position of the tracked satellite, depending on the accuracy of the ground radar.

5.3 Sc. 3: Potential Clouds for the Measure Association Issue

The 5% and 95% potential clouds for two satellites are propagated using validated simulation and the \hat{R}

function (see Equation (4)) with the initial states:

$$\begin{cases} p_1 = 6890939, & p_2 = 6961989, \\ f_1 = 0.0014125, & f_2 = 0.0014182, \\ g_1 = -0.0014160, & g_2 = -0.0014102, \\ h_1 = 0.57763, & h_2 = -0.57763, \\ k_1 = 0.0095098, & k_2 = -0.0095068, \\ L_1 = -0.32425, & L_2 = -0.31903. \end{cases} \quad (14)$$

At last, the trajectories of the two satellites can be compared.

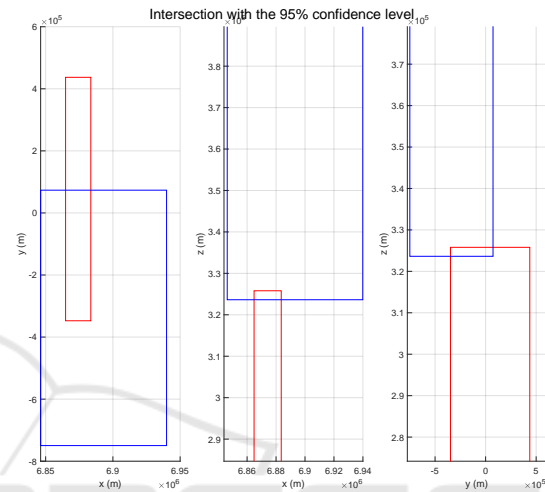


Figure 5: Intersection of position boxes in the ECI frame for the propagation of the 95% potential cloud of two satellites.

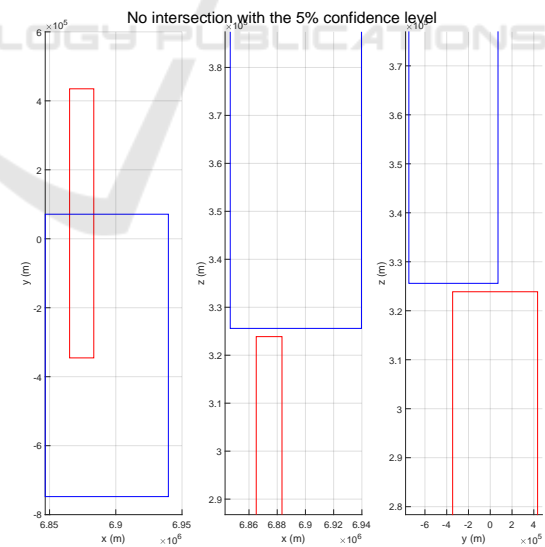


Figure 6: No intersection of position boxes in the ECI frame for the propagation of the 5% potential cloud of two satellites at the same time that Figure 5.

Figures 5 and 6 show a sample of the trajectories where the propagated boxes intersect for a 95% confidence level but not for a 5% confidence level. In that respect, the sensor performances can be evaluated in

terms of required confidence level and decisions can be made depending on this analysis. For example, in that case, if a sensor can only ensure that a collision will never happen with a 5% confidence level, one can decide to use complementary sources of measures in order to improve the estimation of the satellites, or to maneuver one of the satellites in order to increase the confidence level associated to the collision.

6 CONCLUSION AND FUTURE WORKS

In this paper, we proposed a validated algorithm to estimate the trajectory of dynamical systems taking account of uncertainties on the initial state. Our approach uses measures and their uncertainties to quantify likelihood to belong to a certain track. Unlike Monte Carlo methods, our approach provides mathematically guaranteed results that do not ignore low-probability cases, while taking advantage of probability distributions to supplement the information provided by measures. Further, Monte Carlo methods require a substantial number of simulations to be reliable, compared to set-based validated methods which only need one simulation to have as much information with more guarantees.

As future works, implementing the retro-propagation feature of DynIbex to our algorithm would allow using the information given by a measure to reduce the uncertainty of the track beforehand. Moreover, studying the impact of a series of measures depending on the number of measures, the state of the system, the precision of the estimate and the precision of the sensor could help computing the optimal times for taking measures, to gain a maximum of information on the system.

REFERENCES

- Alexandre Dit Sandretto, J. (2019). Confidence-based contractor, propagation and potential cloud for differential equations. *Summer Workshop on Interval Methods 2019*.
- Alexandre dit Sandretto, J. and Chapoutot, A. (2016). Validated Explicit and Implicit Runge-Kutta Methods. *Reliable Computing*, 22.
- Bar-Shalom, Y. and Tse, E. (1975). Tracking in a cluttered environment with probabilistic data association. *Automatica*, 11(5):451–460.
- Benhamou F., Goulard F., G. L. and J-F, P. (1999). Revising hull and box consistency. In *Proceedings of the 16th International Conference on Logic programming*, page 230–244. The MIT Press.
- Blackman, S. and Popoli, R. (1999). *Design and Analysis of Modern Tracking Systems*. Artech House radar library. Artech House.
- Collins, J. and Uhlmann, J. (1992). Efficient gating in data association with multivariate gaussian distributed states. *IEEE Transactions on Aerospace and Electronic Systems*, 28(3):909–916.
- Fortmann, T., Bar-Shalom, Y., and Scheffe, M. (1983). Sonar tracking of multiple targets using joint probabilistic data association. *IEEE journal of Oceanic Engineering*, 8(3):173–184.
- Fuchs, M. and Neumaier, A. (2009). Autonomous robust design optimisation with potential clouds. *Int. J. Reliability and Safety*, 3:23–34.
- Gill, P. E. and Murray, W. (1978). Algorithms for the solution of the nonlinear least-squares problem. *SIAM Journal on Numerical Analysis*, 15(5):977–992.
- Horwood, J. T. and Poore, A. B. (2014). Gauss von mises distribution for improved uncertainty realism in space situational awareness. *SIAM/ASA Journal on uncertainty Quantification*, 2(1):276–304.
- Jaulin, L., Kieffer, M., Didrit, O., and Walter, E. (2001). *Applied Interval Analysis*. Springer London.
- Julier, S. and Uhlmann, J. (2004). Unscented filtering and nonlinear estimation. *Proceedings of the IEEE*, 92(3):401–422.
- Mills-Tettey, G. A., Stentz, A., and Dias, M. B. (2007). The dynamic hungarian algorithm for the assignment problem with changing costs. *Robotics Institute, Pittsburgh, PA, Tech. Rep. CMU-RI-TR-07-27*.
- Nedialkov, N. S., Jackson, K., and Corliss, G. (1999). Validated solutions of initial value problems for ordinary differential equations. *Appl. Math. and Comp.*, 105(1):21 – 68.
- Neyman, J. (1937). Outline of a theory of statistical estimation based on the classical theory of probability. *Phil. Trans. R. Soc. Lond. A*, 236(767):333–380.
- Reid, D. (1979). An algorithm for tracking multiple targets. *IEEE Transactions on Automatic Control*, 24(6):843–854.
- Vallado, D. A. (2001). *Fundamentals of astrodynamics and applications*, volume 12. Springer Science & Business Media.
- Verhagen, S. and Teunissen, P. J. (2017). Least-squares estimation and kalman filtering. In Teunissen, P. J. and Montenbruck, O., editors, *Springer Handbook of Global Navigation Satellite Systems*. Springer International Publishing.
- Walker, M. J., Ireland, B., and Owens, J. (1985). A set modified equinoctial orbit elements (errata 1986). *Celestial mechanics*, 36(4):409–419.